Network disorder and non-affine deformations in marginal solids

Alessio Zaccone, Jamie R. Blundell and Eugene M. Terentjev

Cavendish Laboratory, University of Cambridge, JJ Thomson Avenue, Cambridge CB3 0HE, U.K.

(Dated: January 12, 2012)

The most profound effect of disorder on the elastic response of solids is the non-affinity of local displacements whereby the atoms (particles, network junctions) do not simply follow the macroscopic strain, as they do in perfect crystals, but undergo additional displacements which result in a softening of response. Whether disorder can produce further effects has been an open and difficult question due to our poor understanding of non-affinity. Here we present a systematic analysis of this problem by allowing both network disorder and lattice coordination to vary continuously under account of non-affinity. In one of its limits, our theory, supported by numerical simulations, shows that in lattices close to the limit of mechanical stability the elastic response stiffens proportionally to the degree of disorder. This result has important implications in a variety of areas: from understanding the glass transition problem to the mechanics of biological networks such as the cytoskeleton.

PACS numbers: 62.20.de, 83.80.Fg, 81.05Kf

I. INTRODUCTION

In a disordered lattice subject to a small external deformation, every atom or network junction moves initially in an affine way, that is, displaced in geometric proportion to the macroscopic strain. At the same time, the atom experiences forces from its nearest-neighbors (NN) which are initially displaced affinely too. In any disordered lattice atoms will therefore experience a non-zero force due to the fact that their NN are randomly oriented. By contrast, in a perfectly ordered lattice the forces transmitted by the NN may balance each other by symmetry and the resultant local force in that case can be zero. The finite forces acting on each atom in the disordered network drive additional local displacements, called non-affine displacements[1–3]. As these are accompanied by a release of energy, needed in order to reach mechanical equilibrium on each atom, the effect of non-affinity induced by the disorder on the macroscopic rigidity is always to soften the solid with respect to a purely affine deformation. This softening is a well established phenomenon observed many times in simulations and experimental studies[4,5]. However, since a consistent theoretical description of non-affine elastic response has been elusive so far, it has been difficult to predict the rigidity of disordered solids (including glass, granular media, cytoskeletal networks, etc.) as a function of the degree of structural order/disorder. Apart from its obvious importance for materials science, rigidity is the defining property of the solid state of matter[6] and furthermore the concept of (generalized) rigidity as the epitome of cooperative behavior is essential for various other properties, including how information is transmitted in many-body systems[7]. In spite of this, the relation between rigidity and disorder has remained largely unknown[8]. This may well be the reason for our present lack of understanding of the glass transition phenomenon, wherein rigidity emerges in a (disordered) supercooled liquid without any apparent change in the symmetry of disordered structure[7,9].

Here we report on a systematic theoretical and numerical study of the elastic rigidity (described through the shear modulus) as a function of the degree of structural disorder, which varies from the perfect crystal all the way up to the completely disordered lattice. We focus our analysis to central-force systems[10] where the physical bonds between particles have zero bending rigidity, and to systems which are close to the vanishing of rigidity (*marginal solids*). A wide class of physical systems are captured by these central force models, such as flexibly-linked biological networks and metallic glasses. In some cases, such as covalently bonded materials, junctions can possess bending rigidity which makes the transition to a rigid phase occur at lower connectivity[11–13]. Without loss of generality, our results provide the first direct evidence for the existence of a broad range of structural disorder where increasing the disorder causes lattices near the isostatic limit (i.e. the limit where the number of geometric constraints exactly matches the number of degrees of freedom) to stiffen. This result has deep implications in view of the fact that all liquids on their way toward the solid state do pass through this isostatic limit, whereby even a small difference of mechanical stability with respect to internal stresses generated by vitrification can decide their ultimate fate, i.e. whether to become permanently ordered (crystal) or fully disordered (glass).

II. THE GAUSSIAN BOND-ORIENTATIONAL DISORDER MODEL

Let us start by introducing the bond-orientation vectors between nearest-neighbor atoms i and j defined by $\underline{n}_{ij} = (\cos\phi\sin\theta, \sin\phi\sin\theta, \cos\theta)$. The affine part of the shear modulus of harmonic lattices can be derived from the expansion of the free energy in the harmonic approximation and is given in this limit by the well-known Born-Huang formula[14], for instance, $C^A_{xyxy} = (1/V)\kappa R_0^2 \sum_{ij} c_{ij} n^x_{ij} n^y_{ij} n^x_{ij} n^y_{ij}$, where the lattice sum goes over all nearest-neighbor pairs ij. The atomic force constant κ is defined by the harmonic pair-potential,

$U(r_{ij}) = \frac{1}{2}\kappa(r_{ij} - R_0)^2$, between nearest-neighbors. R_0 is the interatomic distance at rest in the reference frame and V is the volume of the system before deformation. Here and below the Roman indices are used to label atoms while Greek indices are used to label Cartesian components of vectors. c_{ij} is the connectivity matrix with $c_{ij} = 1$ if i and j are nearest neighbors and $c_{ij} = 0$ otherwise in our simple case. Let us consider the shear modulus G of a simple cubic lattice in $d = 3$ in the affine approximation. Every atom has $z = 6$ nearest neighbors and shares a bond with each of them. With N atoms in the lattice, on average each atom contributes $z\langle n_{ij}^x n_{ij}^y n_{ij}^x n_{ij}^y \rangle$ to the lattice sum, where the bond-orientation averaged factor is evaluated with an appropriate, normalized orientation distribution function (ODF) $f(\theta, \phi)$:

$$\langle n_{ij}^x n_{ij}^y n_{ij}^x n_{ij}^y \rangle = \int f(\theta, \phi)\sin^4\theta\cos^2\phi\sin^2\phi \sin\theta d\theta d\phi \tag{1}$$

Using this averaging the Born-Huang formula can be written:

$$C_{xyxy}^A = (1/V)\kappa R_0^2 z \langle n_{ij}^x n_{ij}^y n_{ij}^x n_{ij}^y \rangle. \tag{2}$$

Evaluating $f(\theta, \phi)$ for different physical situations is one of the main exercises of our theory, leading to different forms of the resulting shear modulus. For the simple cubic system, out of the six orientations of the bonds attached to each atom, only two are independent, while the other 4 can be obtained from these by symmetry operations that leave products of n_{ij}^α terms ($\alpha = $ x, y, z) unchanged. These symmetry operations are either rotations (belonging to the octahedral rotation symmetry group O_h) about the zenithal (z-)axis, or reflections through any plane of symmetry of the cubic cell. One of the two independent orientations lies along the zenithal axis and is parameterized by $\theta_{ze} = 0$ and $\forall\phi_{ze}$, while the other one lies in the azimuthal plane and is parameterized by $\theta_{az} = \pi/2$ and $\phi_{az} = 0$ (see Fig.1a). The former occurs with probability 2/6 and the latter one with probability 4/6. Hence the normalized ODF of the simple cubic (SC) lattice can be rewritten, for our purposes, in a simpler normalized form which is going to be used throughout (see the Appendix A for full details): $f_{SC}(\theta, \phi) = (3/2)[(2/6)\delta(\theta) + (4/6)\delta(\theta - \pi/2)\delta(\phi)]$. Using this ODF in Eq.(1) immediately leads to $\langle n_{ij}^x n_{ij}^y n_{ij}^x n_{ij}^y \rangle_{SC} = 0$ and so the affine shear modulus for the SC lattice is $G^A = C_{xyxy}^A = (N/V)z\kappa R_0^2 \langle n_{ij}^x n_{ij}^y n_{ij}^x n_{ij}^y \rangle_{SC} = 0$. This result given by the affine theory for the perfectly ordered simple cubic lattice agrees with Maxwell's counting of degrees of freedom[15] which indeed predicts $G = 0$ for isostatic lattices with $z = 2d = 6$, and also with evidence from polonium-210 in its alpha form, and the superconducting calcium-III, which both feature simple cubic structure and a vanishing shear stability at ambient pressure[16–18].

In the opposite limit of a completely disordered network of harmonic springs, one may assume that all bond
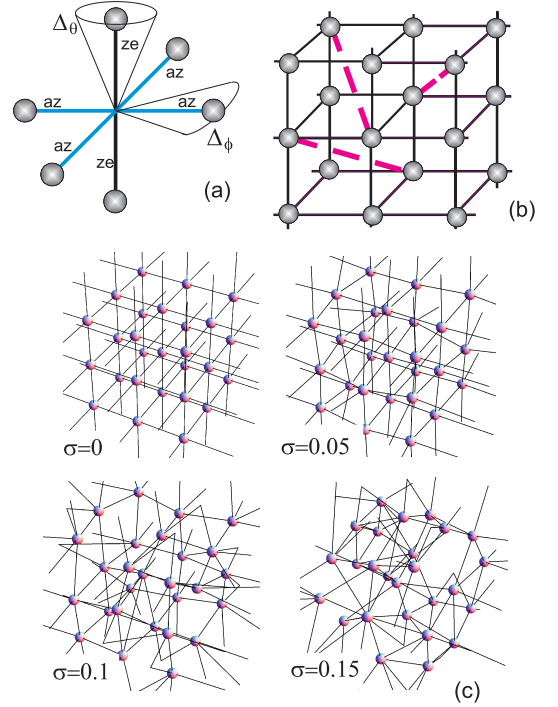

FIG. 1: (a) Primitive cell of the (perfectly ordered) simple cubic lattice. The bonds lying on the horizontal plane are called azimuthal bonds (az); those on the vertical axis are zenithal (ze). (b) Schematic model of cubic lattice with randomly added extra bonds (dashed lines). (c) Marginal solids with varying degree of disorder parameterized by the degree of disorder σ defined in the text.

orientations occur with the same probability. This results in a completely de-correlated (bond-orientational) disorder described by the uniform ODF $f_{UD}(\theta, \phi) = 1/4\pi$ which leads to $\langle n_{ij}^x n_{ij}^y n_{ij}^x n_{ij}^y \rangle_{UD} = 1/15$, where we use the subscript UD for "uniform disorder". Hence using this result in Eq.(2) gives $G = C_{xyxy}^A = (1/30)(N/V)\kappa R_0^2 z$, which is evidently finite for any coordination number z. Thus the affine approximation here dramatically fails to comply with the vanishing of rigidity at isostaticity point (i.e. at $z = 6$), in contrast with both Maxwell's constraint-counting and the empirical evidence[8]. This represents the well-documented failure of the affine approximation to describe the elasticity of disordered lattices[8,19,20].

Let us now introduce a way to quantify arbitrary degrees of structural disorder. We again consider the simple cubic lattice as our starting point and introduce disordered realizations, always keeping $z = 6$ for the time being. The orientations of the bonds now deviate from the cubic lattice axes, and we assume that their distribution is Gaussian about these axes. A particularly convenient choice to parameterize Gaussian bond-orientational disorder in the network of this topology is the following

ODF: $f_{GD} = (2/6)f_{GD}^{ze} + (4/6)f_{GD}^{az}$, with:

$$f_{GD}^{ze} = N_{ze}(\sigma^2)e^{-\theta^2/2\sigma^2}$$
$$f_{GD}^{az} = N_{az}(\sigma^2)e^{-(\theta-\frac{\pi}{2})^2/2\sigma^2}e^{-\phi^2/2\sigma^2} \qquad (3)$$

where the subscript GD stands for "Gaussian disorder" and σ^2 is the variance, which acts as our quantitative measure of lattice disorder. $N_{ze}(\sigma^2)$ and $N_{az}(\sigma^2)$ are normalization factors which also depend on σ^2. We have verified that using this compact form for the ODF, in terms of the two independent directions only, yields quantitatively the same results that one would obtain by considering explicitly all the 6 bond orientations. This ODF allows one to span all intermediate degrees of disorder by varying the parameter σ^2. In the limit $\sigma^2 \to \infty$ this ODF flattens and one recovers the uniform orientational distribution $f_{GD}(\theta, \phi) \to f_{UD}(\theta, \phi) = 1/4\pi$. In the opposite limit of $\sigma^2 \to 0$, delta-functions are developed at the angles of the cubic lattice so that one recovers the simple-cubic ODF, $f_{GD}(\theta, \phi) \to f_{SC}(\theta, \phi)$.

III. ANALYTICAL THEORY OF NON-AFFINE ELASTIC DEFORMATIONS

A. Simple cubic and uniformly disordered lattices

The ultimate cause of non-affinity lies in the fact that the particles bonded to a tagged particle, upon the externally applied strain are initially displaced affinely, and owing to their displacement they exert a net force on the tagged particle. If the particles were placed in an ordered fashion around the tagged particle, such as in crystals, the resultant sum of these forces would be zero due to symmetry. In a disordered solid such a cancelation does not occur. Hence the resultant force is finite, and it induces an additional displacement on the tagged particle in order to keep the mechanical equilibrium, which adds to the affine displacement dictated by the imposed strain. In this way the mechanical equilibrium is preserved on all particles. Clearly, there is a work associated with these non-affine displacements, which bears a negative sign since the overall energy is reduced. Formally this work represents an additional term in the Born free energy expansion and can be written as

$$-W = \sum_i \int_0^{\underline{\mathbf{u}}^{NA}} f_{i\alpha}dx_i^\alpha = -\frac{1}{2}\sum_{ij} H_{ij}^{\alpha\beta}x_i^\alpha x_j^\beta \Big|_{\underline{\mathbf{x}}=\underline{\mathbf{u}}^{NA}}. \qquad (4)$$

The sum runs over all particles and the path integral is over the non-affine displacements $\underline{\mathbf{u}}^{NA}$ which the particle i undergoes under the action of the force field $\underline{f}$ exerted by the neighbors. $H_{ij}^{\alpha\beta} = \partial^2 U/\partial r_i^\alpha \partial r_j^\beta$ is the Hessian matrix and x_i^α are the coordinates of particle i. Then the free energy expansion for a disordered solid accounting for non-affinity is: $\delta F = \delta F_A - W$ where δF_A is the affine (Born) part of the free energy expansion under a
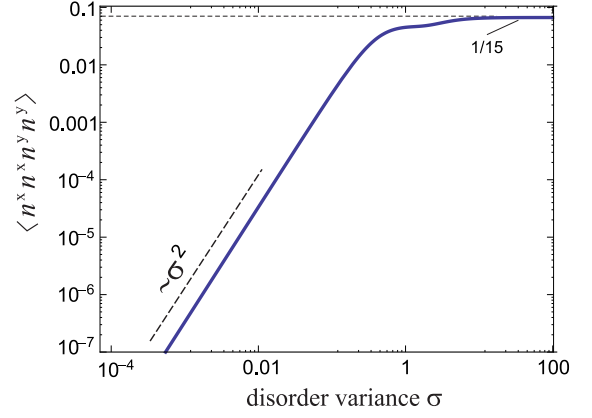

FIG. 2: The theoretical structure-dependent factor in the shear modulus, plotted as a function of the degree of Gaussian disorder σ calculated using Eqs. (1) and (3). The asymptotic value of the strong-disorder plateau and the scaling at weak disorder are shown by dashed lines.

given strain[14], which leads to the Born-Huang formula for the elastic moduli already used above.

The negative non-affine contribution can be handled analytically (further technical details can be found in the Appendix A). It has been recently shown by Lemaitre and Maloney by normal mode decomposition[3] that the non-affine contribution to the modulus takes the form

$$C_{\iota\xi\kappa\chi}^{NA} = \frac{1}{V}\sum_k^{3N} \frac{(\underline{\Xi}_{\iota\xi}\cdot\underline{\mathbf{v}}_k)(\underline{\Xi}_{\kappa\chi}\cdot\underline{\mathbf{v}}_k)}{\lambda_k}, \qquad (5)$$

where $\underline{\Xi}_{\iota\xi}$ are the affine (force) fields acting on each particle, while $\underline{\mathbf{v}}_k$ and λ_k are the eigenvectors (which coincide with the normal modes of the solid) and eigenvalues of the Hessian matrix, respectively. The sum runs over all translational modes (degrees of freedom) of the atoms. Both the affine force fields and the eigenvectors $\underline{\mathbf{v}}_k$ depend on the orientations $\underline{n}_{ij}$ of the bonds in the solid in a way geometrically similar to the way the bonds react elastically (affinely) to the imposed shear deformation. Accordingly, the non-affine term is also proportional to the same $\langle n_{ij}^x n_{ij}^y n_{ij}^x n_{ij}^y \rangle$ factor that has been present in the affine model discussed above. As shown in the Appendix A, an allowed and convenient form of the eigenmodes can be found which leads to the exact evaluation of the non-affine terms in the sum in Eq.(5). Taking the average over the disorder of the terms in the sum leads to $G^{NA} \equiv C_{xyxy}^{NA}$:

$$G^{NA} = (3N)\kappa R_0^2 \langle n_{ij}^x n_{ij}^y n_{ij}^x n_{ij}^y \rangle / V. \qquad (6)$$

The important result is that the non-affine part of the shear modulus is in fact proportional to the same angular average as the affine terms discussed above (because the affine fields which are responsible for the non-affine term have the same dependence on disorder as the affine part), and also to the total number of degrees of freedom

in the network, $3N$, which all take part in the force relaxation. The non-affine effect is, therefore, independent of the connectivity z because the non-affine relaxation involves the degrees of freedom rather than the bonds.

In the limit of uniform disorder we may recall that $G^A = (1/30)(N/V)\kappa R_0^2 z$. Subtracting the corresponding uniform disorder-averaged expression for the non-affine part, G^{NA}, we obtain the shear modulus as

$$G = \frac{1}{30}\frac{N}{V}\kappa R_0^2 z - \frac{1}{15}\frac{3N}{V}\kappa R_0^2 = \frac{N}{30V}\kappa R_0^2(z-6). \quad (7)$$

This equation is derived in the Appendix A. This modulus correctly vanishes at $z = 6$, that is, at the isostatic point of central-force solids where the number of constraints (bonds) equals the number of degrees of freedom. For $z < 6$ there is a finite number of floppy modes and the systems is no longer rigid[15].

Equation (7) is based on the requirement that the Hessian averaged over the orientational disorder be a $3N \times 3N$ matrix where the 3×3 submatrices coincide with the identity matrix, as shown in the Appendix A. This requirement is satisfied for both the simple cubic lattice and the uniformly disordered lattice that have been defined above, i.e. for both the lower and the upper limit of the Gaussian disorder spectrum that we introduced in the previous section. Even though Eq.(7) may not hold exactly for degrees of disorder intermediate between these two limits, we shall continue to assume that Eq.(7) still applies as an approximate relation in between the two limits. In the worst case this may give a reasonable interpolation over the whole disorder spectrum. As this is a rather uncontrolled assumption, it will be tested in comparison with numerical simulations later in this article.

Since the same orientation average $\langle n_{ij}^x n_{ij}^y n_{ij}^x n_{ij}^y \rangle$ appears as a factor in both G^A and G^{NA}, it follows that it plays the same role for an arbitrary degree of disorder, that is, $G \propto \langle n_{ij}^x n_{ij}^y n_{ij}^x n_{ij}^y \rangle_{GD}$, where the average encodes the information about the lattice disorder via $f_{GD}(\theta, \phi)$. The dependence of the microstructure function $\langle n_{ij}^x n_{ij}^y n_{ij}^x n_{ij}^y \rangle_{GD}$ upon the degree of disorder as parameterized by σ^2 is explicitly shown in Fig. 2. In the limit $\sigma^2 \to \infty$, the completely uncorrelated uniform disorder case is recovered, $\langle n_{ij}^x n_{ij}^y n_{ij}^x n_{ij}^y \rangle_{GD} \to 1/15$. In the opposite limit of weak disorder, the structure function goes to zero proportionally to σ^2, recovering the simple-cubic lattice at $\sigma = 0$. The deviation from this proportionality starts to be significant when $\sigma^2 \approx 1$, after which the uniform-disorder plateau ($= 1/15$) sets in.

B. Gaussian bond-orientational disorder with third-body neighbors

We have therefore established that in the simplest situation, where all z NN atoms participate of the same degree of disorder, the effects of coordination and disorder are decoupled and they contribute two distinct factors to the shear modulus, $z - 6$ (the coordination) and $\langle n_{ij}^x n_{ij}^y n_{ij}^x n_{ij}^y \rangle_{GD}$ (the disorder). An important extension arises when bonds between further apart atoms (network junctions) are added on a pre-existing lattice. This situation describes higher coordination networks and occurs, for example, in cytoskeletal networks where filaments are superimposed on an underlying network of a different type of filaments. Clearly, the bond orientations of the added filaments will be distributed differently from the underlying network and thus have a different degree of disorder. In order to capture this extension within our theory, we consider an underlying isostatic network ($z = 2d = 6$) with a variable degree of disorder onto which additional bonds are superimposed and placed at random at the network's junctions. This scheme follows the most common model employed in the study of *marginal solids*[1,22,25] and consists of taking an underlying ordered isostatic lattice and then randomly place additional springs typically connecting next-nearest-neighbor or third-body neighbor atoms (TBN).

Let us identify the bonds belonging to the underlying isostatic lattice as isostatic bonds, while the additional bonds will be referred to as excess bonds (see Fig.1b). On average, out of z bonds per atom there are 6 isostatic bonds of a base cubic lattice, which we assume is formed from the variable (Gaussian) disorder, and $z - 6$ excess bonds per atom. Let us assume the excess bonds are placed between TBN atoms along the diagonal of the cubic cell, so their average length is of the order of $\sqrt{3}R_0$. The four third-body neighbor excess bonds in the upper half-plane are defined by $\theta = \pi/4, \forall \phi$, and $\phi = \pi/4, 3\pi/4, 5\pi/4, 7\pi/4$ while the four TBN bonds in the lower half-plane are parameterized by $\theta = \pi/4 + \pi/2, \forall \phi$, and $\phi = \pi/4, 3\pi/4, 5\pi/4, 7\pi/4$. Hence, on average a randomly placed third-body neighbour contributes a factor proportional to $\langle n_{ij}^x n_{ij}^y n_{ij}^x n_{ij}^y \rangle_{EX} = 0.06944$. This value should be affected by the disorder and thus should vary with σ. However, it is evident that this value can vary only in the very narrow range from 0.06944 (at $\sigma = 0$) to 0.06667 (at $\sigma = \infty$). Therefore, the variation of this term with σ does not lead to a significant change in the shear modulus as a function of σ, also because the σ dependence of the "isostatic" terms is comparatively much stronger. This consideration justifies our setting $\langle n_{ij}^x n_{ij}^y n_{ij}^x n_{ij}^y \rangle_{EX} = const = 0.06944$ independent of σ in the following calculations.

With this decomposition, we can proportionally split the affine part of the shear modulus as $G^A = G_{iso}^A + G_{ex}^A$ where $G_{iso}^A \equiv \frac{1}{2}(N/V)\kappa R_0^2[6/z]z\langle n_{ij}^x n_{ij}^y n_{ij}^x n_{ij}^y \rangle_{GD}$ is due to the isostatic bonds which occur with frequency $6/z$, and $G_{ex}^A \equiv \frac{1}{2}(N/V)\kappa R_0^2[(z-6)/z]z\langle n_{ij}^x n_{ij}^y n_{ij}^x n_{ij}^y \rangle_{UD}$ is due to the excess bonds that occur with frequency $(z-6)/z$. We can similarly split the non-affine contribution into two parts, one due to the 6 isostatic bonds and the second due to the additional $(z - 6)$ randomly placed

TBN bonds:

$$G^{NA} = G_{iso}^{NA} + G_{ex}^{NA} = \frac{1}{2}(N/V)\kappa R_0^2 6 \qquad (8)$$

$$\times \left\{ \frac{6}{z} \langle n_{ij}^x n_{ij}^y n_{ij}^x n_{ij}^y \rangle_{GD} + 3\frac{z-6}{z} \langle n_{ij}^x n_{ij}^y n_{ij}^x n_{ij}^y \rangle_{EX} \right\}$$

We also need to consider a surface term to account for the fact that a finite-size system has the atoms on the surface being displaced affinely as they are constrained to follow the deformation imposed on the box. The frac-

tion of atoms on the surface scales with the total number of atoms as $N^{-2/3}$ (i.e. sub-extensively). It is difficult to precisely determine the number of atoms (the thickness of the surface layer) which follow the strain of the box in a purely affine way. To account for this uncertainty, we introduce a parameter B, of order of unity, and write this additional affine surface term as $G_S^A = \frac{1}{2}(N/V)\kappa R_0^2 z B N^{-2/3} \langle n_{ij}^x n_{ij}^y n_{ij}^x n_{ij}^y \rangle_{GD}$. With all these additional contributions put together, the total shear modulus takes the form:

$$G = \left\{ G_{iso}^A + G_{ex}^A - G_{iso}^{NA} - G_{ex}^{NA} \right\} + G_S^A$$

$$= \frac{1}{2}(N/V)\kappa R_0^2 \left\{ \left[\frac{6}{z}\right](z-6)\langle n_{ij}^x n_{ij}^y n_{ij}^x n_{ij}^y \rangle_{GD} + 3\frac{(z-6)^2}{z} \langle n_{ij}^x n_{ij}^y n_{ij}^x n_{ij}^y \rangle_{EX} \right\} \qquad (9)$$

$$+ \frac{1}{2}(N/V)\kappa R_0^2 z B N^{-2/3} \langle n_{ij}^x n_{ij}^y n_{ij}^x n_{ij}^y \rangle_{GD}.$$

When the number of atoms N is not infinite, the most interesting situation arises for marginal solids as $z \to 6$. In this limit, and in the limit of a large solid ($N \gg 1$) where we can assume that the surface term is negligible, we can also neglect the quadratic term $(z-6)^2$ and have, approximately, $G \approx (N/V)\kappa R_0^2(z-6)\langle n_{ij}^x n_{ij}^y n_{ij}^x n_{ij}^y \rangle_{GD}$ for the non-affine marginal solid with a finite degree of disorder measured by σ. Guided by the Fig.2, we can split the disorder spectrum into a weak disorder regime with $0 < \sigma < 0.1$, and a strong disorder regime with $\sigma > 1$. In the strong disorder regime the shear modulus is practically constant. Remarkably, in this limit our theory recovers the result obtained independently from the numerical analysis of random packings[21] and depleted regular lattices[10]: $G \approx (1/30)(N/V)\kappa R_0^2(z-6)$.

On the other hand, for intermediate and weak disorder the shear modulus is strongly dependent upon the degree of disorder. For weakly disordered cubic networks, with $0 < \sigma < 0.1$, the shear modulus is proportional to σ^2:

$$G \approx 0.175 \frac{N}{V}\kappa R_0^2(z-6)\sigma^2 \qquad (10)$$

If the underlying isostatic lattice is perfectly ordered, i.e. $\sigma = 0$, the general Eq. (9) has the only contribution arising from the excess bonds, giving $G = G_{ex} \propto (z-6)^2$. Remarkably, this scaling agrees with the recent result obtained from the numerical study of square lattices with randomly placed extra springs[22]. We have now seen that the theory predicts that the rigidity of partially disordered lattices near the isostatic point increases upon increasing the degree of structural disorder.

IV. NUMERICAL SIMULATIONS

To test this conclusion, we performed numerical simulations where the disorder is introduced as a perturbation on a reference cubic lattice (Fig.1c). The magnitude of random perturbation for each atom follows the Gaussian distribution with a variance σ^2 along each of the three Cartesian axes. The parameter σ, therefore, controls the degree of quenched disorder in the network, with $\sigma = 0$ corresponding to the cubic lattice and $\sigma \geq 1$ corresponding to a completely disordered lattice. The network topology is formed by introducing z bonds placed at random on the nearest available atoms iteratively, until each atom has z neighbors. A potential energy quadratic in the displacement is associated with every bond and the total free energy is computed by adding the contributions from all the bonds. One should note that the perturbation of the lattice leads to bond lengths that differ from the equilibrium length R_0, an effect which is not considered by the theory. However, the contributions from all the bonds are summed up and therefore the contributions of shorter and longer (than R_0) bonds compensate each other yielding something not dissimilar from the equilibrium bond length upon summing up the contributions. A further consequence of assuming that all bonds are at the equilibrium length is the automatic vanishing of the first-order terms in the free-energy Born expansion. These terms are related to internal stresses but also in this case, upon averaging over the whole network, the various contributions cancel to give a small net contribution (a well-documented fact in the glass simulation literature, see e.g. Tanguy et al.[4]). In weakly connected systems (where $z < 6$ and bond-bending interactions are active) the situation might be different as discussed in
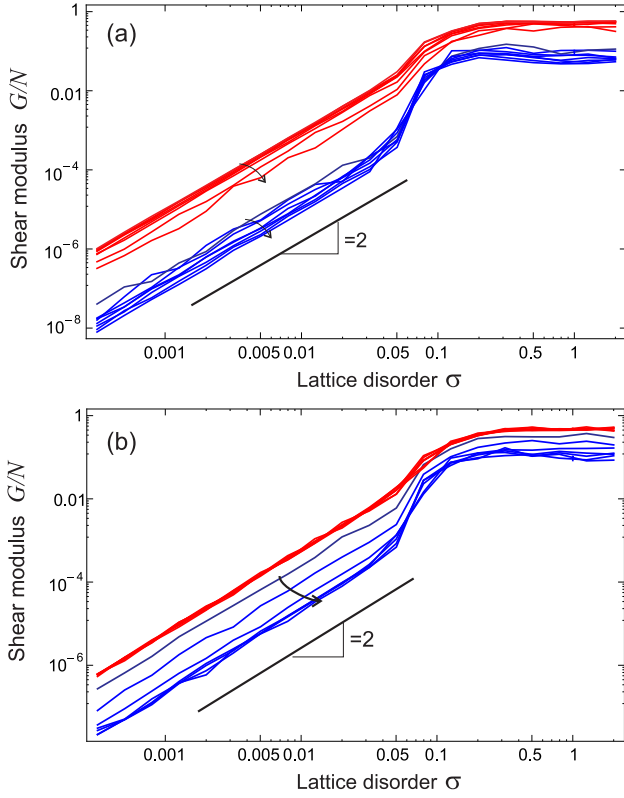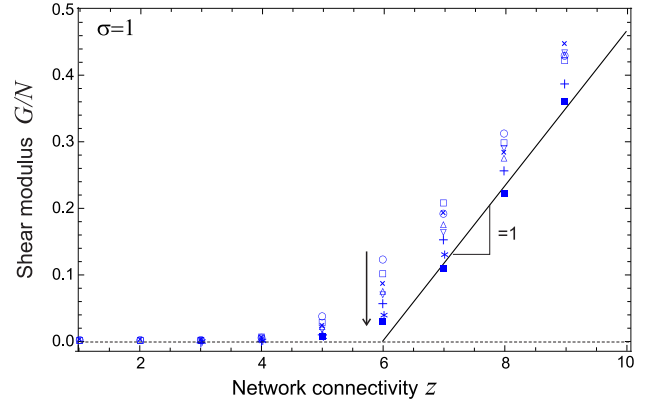
FIG. 4: The shear modulus of simulated networks, for a fixed value of the disorder variance $\sigma = 1$, plotted as a function of connectivity z, taking only integer values in this simulation. The arrow indicates the direction of increasing number of particles: the lattice size from top to bottom is $N = 4^3, 5^3, 6^3, 8^3, 10^3, 12^3, 15^3$ and 20^3. The solid line is the theoretical scaling[19] $G \sim (z - 6)$, valid for $z \to 6$.

plateau at $\sigma \approx 1$. Further, it is seen that non-affinity causes a substantial softening of the solid (lower shear modulus) with respect to the purely affine case even though the dependence upon σ is the same for both affine and non-affine simulations. Varying the connectivity at a fixed degree of disorder, the simulated networks display a rigidity transition at the isostatic point. As shown in Fig.4, the fundamental scaling $G \propto (z - 6)$ due to non-affinity is asymptotically approached in the large N limit. In Fig.5 theory and simulation results are shown together as a function of the degree of disorder upon varying the connectivity. The theory is in fairly good agreement with the simulations for both $z = 6$ and $z = 7$. It should be noted that the surface term (G_S^A in Eq. (9)) plays an essential role in this comparison because it ensures that the solid remains *marginally* rigid with N finite also at $z = 6$. Further, it is seen that upon increasing the connectivity z above the marginal-solid limit ($z = 6$) the shear modulus becomes gradually less sensitive to disorder and eventually becomes independent of σ. This is another important and new result: the rigidity of central-force lattices with $z \geq 7$ is very little affected by the degree of structural order/disorder of the lattice. In the window of disorder $0.05 < \sigma < 0.5$ the theory appears to underestimate the simulation data which exhibit a large hump before reaching the plateau corresponding to strong disorder. Although there can be many reasons for this disagreement, the simulation being completely independent, and using a subtly different way to define disorder σ, one possibility also lies in the assumption (Appendix A) that the submatrices of the Hessian which determine the form of the eigenvectors (required to calculate the non-affine term) reduce to identity matrices upon averaging, which is an exact procedure only for the two opposite SC and UD limits. We have thus shown that the rigidity of a cubic lattice increases upon
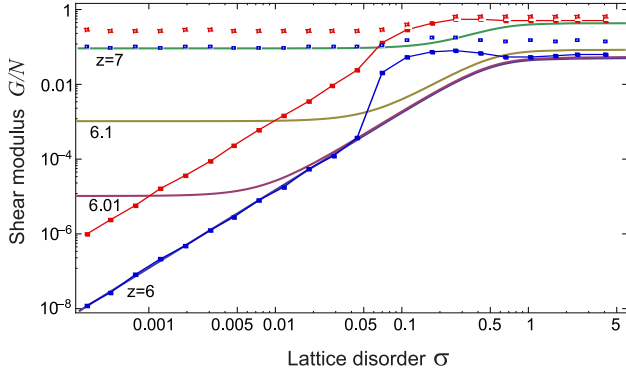
FIG. 3: The shear modulus of simulated isostatic networks ($z = 6$) as a function of the disorder variance σ. Red lines: affine, blue lines: non-affine results. In plot (a) the arrows show the curves changing with the increasing network size, $N = 4^3, 5^3, 6^3, 7^3, 8^3, 9^3$ and 10^3, respectively. In plot (b) the arrows show the convergence of simulation (N=216 as an example) for increasing number of steps, $t = 10, 30, 100, 1000, 10^4, 310^4$ and 10^5.

earlier works (e.g.[1]).

Upon submitting the system to small external deformations of simple shear, the mechanical equilibrium condition on each atom/node is enforced such that it follows the imposed deformation by moving along paths of minimum mechanical energy. This implies, in turn, that each atom moves non-affinely in response to the external strain (see Appendix C for detail). From the total free energy computed in this way we measure the shear modulus of the lattices upon varying the degree of disorder σ and the connectivity z. The results are reported in Fig.3. First of all, these plots confirm that our simulations are valid, both in terms of the scaling $G/N \sim N^{-2/3}$ of Eq.(9) (Fig.3a) and the convergence to equilibrium (Fig.3b) tested. It is especially instructive to note that when only a short time is allowed for force relaxation, the non-affine modulus is very close to the affine result.

The simulation results reproduce the fundamental laws predicted by the theory, as summarized in Eq. (9). For the isostatic (marginal-solid) limit with $z = 6$, and for low to moderate disorder, the shear modulus increases in proportion to σ^2, and then reaches a strong-disorder

FIG. 5: The shear modulus from the analytical theory (solid lines) and simulations (open symbols) upon varying both disorder variance, σ, and lattice connectivity, z. Red symbols refer to the affine moduli, blue symbols to the moduli accounting for non-affinity, for the two discrete cases $z = 6$ and $z = 7$. The continuous variation of z above the isostatic point $z = 6$ shows how the effect of disorder diminishes, and gradually disappears at higher connectivity.

introducing structural bond-orientational disorder, with a law of direct proportionality to the disorder variance. Clearly, the disorder-induced stiffening is an effect controlled by the orientation average $\langle n_{ij}^x n_{ij}^y n_{ij}^x n_{ij}^y \rangle$, which has a simple geometrical meaning: it measures the extent to which the bond-vectors of the lattice are misaligned with respect to the shear-deformation axes, x and y. In fact, the product $\langle n_{ij}^x n_{ij}^y n_{ij}^x n_{ij}^y \rangle$ vanishes for the simple cubic lattice where all bonds are parallel to either the x or the y axis. On the other hand, the product $\langle n_{ij}^x n_{ij}^y n_{ij}^x n_{ij}^y \rangle$ is maximized and saturates to its highest value ($=1/15$) when the bonds tend to be randomly oriented. In the cubic lattice the vanishing of $\langle n_{ij}^x n_{ij}^y n_{ij}^x n_{ij}^y \rangle$ and the shear modulus with it, reflects the fact that there is no restoring force if all parallel columns in either the x or y direction are tilted (maintaining the constant separation of neighbors), which is an example of a floppy mode. In disordered lattices, with bonds misaligned with respect to x and y, the longitudinal components of the bond displacements cannot be neglected (they are no longer second order with respect to the displacement magnitude) which implies a finite restoring force and thus a finite shear modulus. From a different perspective, the factor $\langle n_{ij}^x n_{ij}^y n_{ij}^x n_{ij}^y \rangle$ measures the average local (geometric) frustration of the bonds and it takes a finite value whenever the bonds no longer can be displaced without paying a finite energy cost.

V. CONCLUSIONS

First of all, the conclusion that bond-orientational disorder causes stiffening of an ordered lattice can be extended to other crystal lattices by re-evaluating the factor $\langle n_{ij}^x n_{ij}^y n_{ij}^x n_{ij}^y \rangle$. For example, for the hexagonal close

packed (hcp) lattice with $z_{HCP} = 12$ we find that

$$\langle n_{ij}^x n_{ij}^y n_{ij}^x n_{ij}^y \rangle_{HCP} = \frac{1}{16\pi} \left(\frac{27\sqrt{3}+3}{512} \right) \approx 0.0019. \quad (11)$$

As a result, the ratio between the hcp modulus and the modulus of a uniformly disordered z-coordinated lattice takes the form:

$$\frac{G_{HCP}}{G_{UD}} = \frac{\langle n_{ij}^x n_{ij}^y n_{ij}^x n_{ij}^y \rangle_{HCP}}{\langle n_{ij}^x n_{ij}^y n_{ij}^x n_{ij}^y \rangle_{UD}} \approx 0.0285 \frac{z_{HCP}}{z-6}, \quad (12)$$

where we used that $G_{NA} \equiv 0$ for the ideal hcp lattice. If, for instance, the disordered lattice has $z = 7$, then $G_{HCP}/G_{UD} \approx 1/3$, i.e. the shear modulus of an ideal hcp lattice with $z = 12$ (for which the non-affinity is certainly negligible) is almost three times smaller than the shear modulus of a lattice with uniform disorder and $z = 7$, in spite of the hcp lattice being more strongly connected. The difference becomes more pronounced upon increasing the coordination of the disordered lattice. Therefore the disorder-induced stiffening of crystal lattices is a general effect not limited to the cubic lattice studied in detail above.

Secondly, these findings may have consequences for the glass transition of supercooled liquids. Descriptive theories of the glass transition have emphasized the role of local icosahedral symmetry which emerges at the glass transition[26]. Icosahedral clusters have also been identified with the cooperatively rearranging regions of mean-field (e.g. Adam-Gibbs) theories[27]. The growth and jamming of such icosahedral clusters lead to the sudden increase of the viscosity and eventually to the structural arrest. In the icosahedral clusters an atom at the center is bonded to its 12 nearest neighbors, forming an icosahedron where none of the bonds can be parallel with either the x or y directions. Instead, clusters with hcp symmetry could be formed which have the same number of bonds as the icosahedra but 6 of these bonds can be aligned with the x and y axis. The same applies to fcc clusters. Therefore it follows that the factor $\langle n_{ij}^x n_{ij}^y n_{ij}^x n_{ij}^y \rangle$ is much larger for the icosahedra than for either hcp or fcc clusters and thus the icosahedra are more rigid than the hcp or fcc clusters. This implies that, during the supercooling process, the icosahedra, which are the precursor of the rigid glass state[28], are able to stand the internal stresses generated by the vitrification[1] better than the hcp or fcc clusters which are the precursor of the ordered crystal. This is an unprecedented observation that sheds light on the physical origin of the onset of rigidity at the glass transition.

In further developments, this theory can be applied to analyze the onset of rigidity in systems which possess medium-range order[29], such as the technologically important amorphous semiconductors and metallic glasses[30,31]. In principle, the orientation distribution function for partially disordered lattices (e.g., those containing defects such as dislocations causing distortion of the bond-orientations, or the above mentioned solids with medium-

range order) can be extracted from structural investigation of the material in question (e.g., scattering or microscopy techniques) and used as input in our theory to investigate the elastic properties as a function of structure.

In summary, by combining theory and simulations we have established a fundamental law which governs the rigidity of solids as a function of structural disorder. According to this law, the stiffness of lattices increases with the degree of bond-orientational disorder. Our finding suggests a new way of increasing the mechanical stability of technologically important marginal-solids such as e.g. Po^{210} and the superconducting Ca-III, both of which exhibit simple cubic lattices which therefore can be stabilized by introducing structural disorder (e.g. in the form of defects). Furthermore, our findings suggest a new way of looking at the unresolved problem of the glass transition. In light of our results, vitrifying liquids upon crossing the marginal-solidity or isostatic threshold find themselves in disordered configurations which are intrinsically more rigid than the ordered ones.

Acknowledgments.

Appendix A: Non-affine deformations

In the following we give a brief outline of the analytical method that we devised to calculate the elastic constants of disordered harmonic lattices which accounts for non-affinity[3,19]. The method makes use of the non-affine linear response formalism for disordered solids which is described in detail by Lemaitre and Maloney[3]. One of the central results of the formalism, which represents the starting point of our derivation, is the exact lattice sum for the elastic moduli accounting for non-affinity[3]

$$C_{\iota\xi\kappa\chi} = C_{\iota\xi\kappa\chi}^{A} - C_{\iota\xi\kappa\chi}^{NA} \tag{A1}$$

$$= \frac{R_0^2 \kappa}{2V} \sum_{ij} c_{ij} n_{ij}^{\iota} n_{ij}^{\kappa} n_{ij}^{\xi} n_{ij}^{\chi} - \frac{1}{V} \sum_{k}^{3N} \frac{(\underline{\Xi}_{\iota\xi} \cdot \mathbf{v}_k)(\underline{\Xi}_{\kappa\chi} \cdot \mathbf{v}_k)}{\lambda_k}$$

The superscripts A and NA denote the affine and non-affine parts of the moduli, respectively. The affine part is the standard Born-Huang expression in terms of a lattice sum over nearest-neighbors (NN) i and j, where $\underline{n}_{ij} = (\cos\phi\sin\theta, \sin\phi\sin\theta, \cos\theta)$ is the unit vector defining the orientation of bond ij. c_{ij} is the adjacency matrix ($c_{ij} = 1$ for two NN atoms and $c_{ij} = 0$ otherwise) and κ the harmonic spring constant of the harmonic interaction between two NN atoms. The non-affine part is a

sum over the $3N$ eigenmodes of the Hessian or dynamical matrix of the lattice. The $3N \times 3N$ Hessian matrix for harmonic lattices is given by

$$H_{ij}^{\alpha\beta} = \delta_{ij} \sum_{s} \kappa c_{is} n_{is}^{\alpha} n_{is}^{\beta} - (1 - \delta_{ij}) \kappa c_{ij} n_{ij}^{\alpha} n_{ij}^{\beta} \tag{A2}$$

Eq.(A2) follows from replacing the harmonic potential $U(r_{ij}) = \frac{1}{2}\kappa(r_{ij} - R_0)^2$ in the definition of the Hessian matrix: $H_{ij}^{\alpha\beta} \equiv \partial^2 U / \partial r_i^{\alpha} \partial r_j^{\beta}$. R_0 is the rest length of the bonds. $\mathbf{v}_k$ and λ_k in Eq.(A1) are eigenvectors and eigenvalues of the Hessian, respectively. The inner product $(\underline{\Xi}_{\iota\xi} \cdot \mathbf{v}_k)$ is the projection of the affine force field $\underline{\Xi}_{\iota\xi}$ (i.e., the force field exerted on every atom by the affine motions of its neighbours) on the eigenvector $\mathbf{v}_k$. The analytical form of the affine fields is given by[3]: $\Xi_{i,\kappa\chi}^{\alpha} = -\sum_{j} R_{ij}\kappa c_{ij} n_{ij}^{\alpha} n_{ij}^{\kappa} n_{ij}^{\chi}$. Thus, the evaluation of the non-affine term in the elastic moduli reduces to the task of evaluating the eigenmodes of the Hessian, $\mathbf{v}_k = \underline{a}_r \otimes \underline{w}_l$ where $r = 1...N$ and $l = x, y, z$. In general, there are no analytical routes to evaluate the eigenmodes. This becomes possible however if one chooses $\underline{w}_l = \underline{e}_l$ where $\underline{e}_l$ is the standard Cartesian basis of $\mathbb{R}^3$, as we show below. This treatment is exact in the case of the simple cubic (SC) lattice where the Hessian is exactly given by $H_{ij}^{\alpha\beta} = \frac{\kappa}{3}\left(\delta_{ij}\sum_{j} c_{ij} - (1 - \delta_{ij})c_{ij}\right)\delta_{\alpha\beta}$ and clearly the $\mathbf{v}_k = \underline{a}_r \otimes \underline{e}_l$ are eigenvectors of the Hessian because the submatrices of the Hessian are diagonal. In the case of the uniformly disordered (UD) (isotropic) lattice as defined in the main article, it can be shown that the eigenvectors have the same form. A general theorem states that if $\mathbf{v}_k$ and λ_k are respectively the eigenvectors and eigenvalues of a matrix $\underline{A}$, the same eigenvectors are shared by a matrix $f(\underline{A})$, for any function f of the matrix. The eigenvalue equation for the latter matrix is then given by: $f(\underline{A})\mathbf{v}_k = f(\lambda_k)\mathbf{v}_k$. Let us take $f(...) = \langle...\rangle$, where $\langle...\rangle$ denotes the average over the bond-orientational disorder, as usual. Then we have $f(\underline{H}) = \frac{\kappa}{3}\left(\delta_{ij}\sum_{j} c_{ij} - (1 - \delta_{ij})c_{ij}\right)\delta_{\alpha\beta}$, where $\delta_{\alpha\beta}$ is the Kronecker's delta. Furthermore, $\lambda_k = m\omega_k^2$ where ω_k are the normal mode frequencies of the solid. The lattice with uniform disorder is an isotropic solid, which means that the normal mode frequencies depend only on scalar quantities. Clearly the same applies to the λ_k which in turn implies: $f(\lambda_k) = \lambda_k$. This result establishes that the eigenvectors of the form: $\mathbf{v}_k = \underline{a}_r \otimes \underline{e}_l$ are also eigenvectors of the Hessian for the uniformly disordered lattice. Hence, in both the SC and UD limits one can write the eigenvalue equation for the Hessian as: $(\underline{\tilde{H}} \otimes \underline{I})(\underline{a} \otimes \underline{e}) = \lambda(\underline{a} \otimes \underline{e})$, where $\underline{\tilde{H}} \equiv \frac{\kappa}{3}\left(\delta_{ij}\sum_{j} c_{ij} - (1 - \delta_{ij})c_{ij}\right)$ and $\underline{I}$ denotes the 3×3 identity matrix. Then the inner products of the affine fields with the eigenmodes become[19]:

$$(\underline{\Xi}_{\iota\xi} \cdot \mathbf{v}_k) = \tag{A3}$$

$$= \kappa^2 R_0^2 \sum_{rs,r's'} a_r a_{r'} c_{rs} c_{r's'} n_{rs}^{l} n_{rs}^{\iota} n_{rs}^{\xi} n_{r's'}^{l} n_{r's'}^{\kappa} n_{r's'}^{\chi}$$

where the sum runs over two pairs of NN atoms at the time, rs and $r's'$. Consistent with the main approximation of this theory, we replace the orientation-dependent terms with their orientation average. One finds that $\langle n_{rs}^l n_{rs}^\iota n_{rs}^\xi n_{r's'}^l n_{r's'}^\kappa n_{r's'}^\chi \rangle = (\delta_{rr'}\delta_{ss'} - \delta_{rs}\delta_{sr'})B_{l,\iota\xi\kappa\chi}$ where $B_{l,\iota\xi\kappa\chi} = \langle n_{ij}^\iota n_{ij}^\xi n_{ij}^\kappa n_{ij}^\chi \rangle$ and $\langle ... \rangle = \int ...f(\theta,\phi)\sin\theta d\theta d\phi$ denotes the average over bond orientations according to some orientation distribution function $f(\theta,\phi)$. Replacing this average in Eq.(A3), one obtains:

$$(\underline{\Xi}_{\iota\xi} \cdot \mathbf{v}_k)(\underline{\Xi}_{\kappa\chi} \cdot \mathbf{v}_k) = \qquad (A4)$$
$$= \kappa^2 R_0^2 B_{l,\iota\xi\kappa\chi}\left(\sum_{rs} a_r^2 c_{rs}c_{rs} - \sum_{rs} a_r a_s c_{rs}c_{sr}\right)$$

Furthermore, we have that $c_{rs}^2 = c_{rs}c_{sr} = c_{rs}$ and the identities $\sum_r^N a_r^2 \sum_s c_{rs} - \sum_{rs} a_r a_s c_{rs} = \sum_{rs}^N a_r a_s[(\sum_j^N c_{rj})\delta_{rs} - c_{rs}(1-\delta_{rs})] = \frac{3}{\kappa}\sum_{rs}^N a_r a_s \tilde{H}_{rs}$, where we defined $\underline{\underline{H}} = \underline{\underline{\tilde{H}}} \otimes \underline{I}$ and $\underline{I}$ is the 3×3 identity matrix. Recalling that $\sum_s^N \tilde{H}_{rs} a_s = \lambda a_r$ we obtain $(\underline{\Xi}_{\iota\xi} \cdot \mathbf{v}_k)(\underline{\Xi}_{\kappa\chi} \cdot \mathbf{v}_k) = \kappa R_0^2 \lambda_k B_{l,\iota\xi\kappa\chi}$ Using this result in Eq.(A1), the non-affine part of the shear modulus follows as:

$$G^{NA} \equiv \frac{1}{V}\sum_k^{3N} \frac{(\underline{\Xi}_{xy} \cdot \mathbf{v}_k)(\underline{\Xi}_{xy} \cdot \mathbf{v}_k)}{\lambda_k}$$
$$= \frac{1}{V}\sum_{k=1}^N \sum_{l=1}^3 \frac{3\kappa R_0^2 \lambda_k B_{l,\iota\xi\kappa\chi}}{\lambda_k} \qquad (A5)$$
$$= 3N\kappa R_0^2 \langle n_{ij}^x n_{ij}^y n_{ij}^x n_{ij}^y \rangle / V$$

which is a key result used in the main part of the article.

This theory strictly applies to the SC and UD limits only because only in these specific cases the angular average $\langle n_{ij}^\alpha n_{ij}^\beta \rangle = \delta_{\alpha\beta}/3$ is exact. However, we make the additional assumption that for the intermediate degrees of disorder this result still holds approximately, i.e. $\langle n_{ij}^\alpha n_{ij}^\beta \rangle \simeq \delta_{\alpha\beta}/3$ for $0 < \sigma < \infty$. Within this approximation Eq.(A5) can be used to evaluate the elastic moduli of lattices with disorder (parameterized by variable σ), by using the Gaussian ODF defined in the main article

to evaluate the orientation average in Eq.(A5). In the worst situation, this approximation still should provide a reasonable interpolation since it correctly describes both the lower (SC) and upper (UD) limits of the disorder spectrum. The validity of the approximation has been checked by comparison with simulation data in the main article and as expected it provides a good description of the data apart for a window of disorder $0.05 < \sigma < 0.5$ located in the middle of the spectrum.

Appendix B: Gaussian disorder

The distribution function for the orientation of the lattice bonds (ODF) $f(\theta,\phi)$ is defined by the following relation

$$\langle ... \rangle = \int ...f(\theta,\phi)\sin\theta d\theta d\phi \qquad (B1)$$

To evaluate the shear modulus we need to evaluate its structure-dependent part

$$\langle n_{ij}^x n_{ij}^y n_{ij}^x n_{ij}^y \rangle = \int f(\theta,\phi)\sin^4\theta\cos^2\phi\sin^2\phi \sin\theta d\theta d\phi \qquad (B2)$$

All the information about the structure of the lattice is contained in $f(\theta,\phi)$. For isostatic lattices in $d = 3$, as explained in the main body of the article, the degree of structural disorder can be varied continuously from the simple cubic lattice to the complete uncorrelated disorder by using the following Gaussian ODF

$$f_{GD}(\theta,\phi) = \frac{2}{6}f_{GD}^{ze}(\theta,\phi) + \frac{4}{6}f_{GD}^{az}(\theta,\phi) \qquad (B3)$$

with

$$f_{GD}^{ze}(\theta,\phi) = N_{ze}(\sigma^2)e^{-\theta^2/2\sigma^2}$$
$$f_{GD}^{az}(\theta,\phi) = N_{az}(\sigma^2)e^{-(\theta-\pi/2)^2/2\sigma^2}e^{-\phi^2/2\sigma^2} \qquad (B4)$$

The normalization factors N_{ze} and N_{az} are defined by

$$\int N_{ze}(\sigma^2)f_{GD}^{ze}(\theta,\phi)\sin\theta d\theta d\phi = 1$$
$$\int N_{az}(\sigma^2)f_{GD}^{az}(\theta,\phi)\sin\theta d\theta d\phi = 1 \qquad (B5)$$

Combining Eq.(B3)-(B5) we obtain the following analytical expression for the microstructure-dependent factor in the shear modulus:

$$\langle n_{ij}^x n_{ij}^y n_{ij}^x n_{ij}^y \rangle_{GD} = \int f_{GD}(\theta,\phi)\sin^4\theta\cos^2\phi\sin^2\phi\,\sin\theta d\theta d\phi$$
$$= \{e^{-12\sigma^2}\sqrt{1/\sigma^2}\sqrt{\sigma^2}(\text{Erf}[(\pi-5i\sigma^2)/\sqrt{2\sigma^2}] + \text{Erf}[(\pi+5i\sigma^2)/\sqrt{2\sigma^2}]$$
$$+5e^{8\sigma^2}(\text{Erf}[(\pi-3i\sigma^2)/\sqrt{2\sigma^2}] - \text{Erf}[(\pi+3i\sigma^2)/\sqrt{2\sigma^2}]$$
$$-2e^{4\sigma^2}(\text{Erf}[(\pi-i\sigma^2)/\sqrt{2\sigma^2}] - \text{Erf}[(\pi+i\sigma^2)/\sqrt{2\sigma^2}] + 2i\text{Erfi}[\sqrt{\sigma^2/2}])$$
$$+2i\text{Erfi}[(3\sqrt{\sigma^2})/\sqrt{2}]) - 2i\text{Erfi}[5\sqrt{\sigma^2}/\sqrt{2}])\}$$
$$\times \{384(\text{Erf}[((\pi+i\sigma^2)\sqrt{1/2\sigma^2}] - 2i\text{Erfi}[1/\sqrt{2/\sigma^2}]$$
$$+i\text{Erfi}[(\sqrt{1/\sigma^2}(i\pi+\sigma^2))/\sqrt{2}])\}^{-1}$$
$$+ \{e^{-20\sigma^2}(5e^{8\sigma^2}(2e^{4\sigma^2}(\text{Erf}[(\pi-2i\sigma^2)/2\sqrt{2\sigma^2}] + \text{Erf}[(\pi+2i\sigma^2)/2\sqrt{2\sigma^2}])$$
$$+\text{Erf}[(\pi-6i\sigma^2)/(2\sqrt{2\sigma^2})] + \text{Erf}[(\pi+6i\sigma^2)/(2\sqrt{2\sigma^2})])$$
$$+\text{Erf}[(\pi-10i\sigma^2)/(2\sqrt{2\sigma^2})]$$
$$+\text{Erf}[(\pi+10i\sigma^2)/(2\sqrt{2\sigma^2})])(-2+2e^{8\sigma^2}\text{Erf}[(\sqrt{2}\pi)/\sqrt{\sigma^2}]$$
$$+\text{Erfc}[(\sqrt{2}(\pi-2i\sigma^2))/\sqrt{\sigma^2}] + \text{Erfc}[(\sqrt{2}(\pi+2i\sigma^2))/\sqrt{\sigma^2}]))\}$$
$$\times \{768\text{Erf}[\pi/\sqrt{2\sigma^2}](\text{Erf}[(\pi-2i\sigma^2)/2\sqrt{2\sigma^2}]$$
$$+\text{Erf}[(\pi+2i\sigma^2)/(2\sqrt{2\sigma^2})])\}^{-1} \tag{B6}$$

Eq.(B6) is a function of the Gaussian variance σ^2 only and has been plotted in Fig.2 in the main body of the article.

Derivation of the Gaussian ODF

Here we provide a proof of the expression given by Eq.(2) in the main article (Eqs.(B3)-(B4) in the section above) for the Gaussian ODF used to vary the degree of disorder in our model. We start by considering the orientations of the bonds in the primitive cell of the simple cubic (SC) lattice. There are 4 bonds lying in the xy plane that are defined by pairs (θ,ϕ) of angles $(\pi/2,0)$, $(\pi/2,\pi/2)$, $(\pi/2,\pi)$, and $(\pi/2,3\pi/2)$. Further, there are two bonds lying along the polar z-axis defined by $(0,\forall\phi)$ and $(\pi,\forall\phi)$. The Gaussian model realizes the situation where each of these bonds is distributed around the simple-cubic angle pairs mentioned above according to a Gaussian distribution f_{GD} with variance σ^2. In the limit $\sigma \to 0$ the model develops Dirac deltas at the SC bond orientations thus recovering the perfectly ordered SC lattice. We wish to demonstrate that in order to evaluate the angular average $\langle n_{ij}^x n_{ij}^y n_{ij}^x n_{ij}^y \rangle_{GD} = \int ...f_{GD}(\theta,\phi)\sin\theta d\theta d\phi$, one needs only to consider the two principal orientations $(\pi/2,0)$ and $(0,\forall\phi)$ (from which the other ones can be obtained upon application of the symmetry operations of the group O_h), which we denote as *azimuthal* and *zenithal* respectively, because all the other orientations contribute terms which are identical to either of these two. In other words, we want to show that for the purpose of evaluating $\langle n_{ij}^x n_{ij}^y n_{ij}^x n_{ij}^y \rangle_{GD}$ the following identities hold:

$$f_{GD} \equiv \frac{1}{6}\left(\sum_{p=0}^{3} f_{GD}^{\{\frac{\pi}{2},p\frac{\pi}{2}\}} + \sum_{q=0}^{1} f_{GD}^{\{q\pi,\forall\phi\}}\right) = \frac{4}{6}f_{GD}^{az} + \frac{2}{6}f_{GD}^{ze} \tag{B7}$$

where we identified:

$$f_{GD}^{az} \equiv f_{GD}^{\{\frac{\pi}{2},0\}} \equiv N_{az}(\sigma^2)e^{-(\theta-\frac{\pi}{2})^2/2\sigma^2}e^{-\phi^2/2\sigma^2}$$
$$f_{GD}^{ze} \equiv f_{GD}^{\{0,\forall\phi\}} \equiv N_{ze}(\sigma^2)e^{-\theta^2/2\sigma^2} \tag{B8}$$

i.e. the first terms of the two sums in Eq.(B7), defined by $p = 0$ and $q = 0$, respectively. Let us start with the orientations in the xy plane. The principal azimuthal orientation f_{GD}^{az}, with $p = 0$, contributes to the average $\langle n_{ij}^x n_{ij}^y n_{ij}^x n_{ij}^y \rangle_{GD}$ the following integral:

$$\int \sin^4\theta\cos^2\phi\sin^2\phi e^{-(\theta-\frac{\pi}{2})^2/2\sigma^2}e^{-\phi^2/2\sigma^2}\sin\theta d\theta d\phi$$

$$+ \int \sin^4\theta\cos^2\phi\sin^2\phi e^{-(\theta-\frac{\pi}{2})^2/2\sigma^2}e^{-(\phi-2\pi)^2/2\sigma^2}\sin\theta d\theta d\phi$$

$$= 2\int \sin^4\theta\cos^2\phi\sin^2\phi e^{-(\theta-\frac{\pi}{2})^2/2\sigma^2}e^{-\phi^2/2\sigma^2}\sin\theta d\theta d\phi \tag{B9}$$

where we omitted the normalization factor and where the equality holds because the functions in the two integral on the l.h.s. subtend the same area within the same interval of integration $[0,2\pi]$. It should be noted that the second term on the l.h.s. is strictly required in order to have a Gaussian centered on $\phi = 0$. Without this term, since integration goes from 0 to 2π, one would have only half of the Gaussian and would not properly count the contributions from the angles which lie close to $\phi = 2\pi$ (or equivalently on the negative axis close to $\phi = 0^-$).

The second term in the first sum in Eq.(B7), with $p = 1$, contributes to the average the following term:

$$\int_0^\pi \sin^5\theta e^{-(\theta-\frac{\pi}{2})^2/2\sigma^2}d\theta \int_0^{2\pi}\cos^2\phi\sin^2\phi e^{-(\phi-\frac{\pi}{2})^2/2\sigma^2}d\phi \tag{B10}$$

In this integral, let us change to the variable $\Phi \equiv \phi - \frac{\pi}{2}$. Upon applying the well-known trigonometric relations: $\sin(\phi+\frac{\pi}{2}) = \cos\phi$ and $\cos(\phi+\frac{\pi}{2}) = -\sin\phi$, the integral

in Eq.(B10) becomes:

$$\int_0^\pi \sin^5\theta e^{-(\theta-\frac{\pi}{2})^2/2\sigma^2} d\theta \int_{-\frac{\pi}{2}}^{\frac{3\pi}{2}} \cos^2\Phi\sin^2\Phi e^{-\Phi^2/2\sigma^2} d\Phi$$

$$(B11)$$

This integral is identical to the r.h.s. of Eq.(B9) because the area subtended by the function $\cos^2\phi\sin^2\phi e^{-\phi^2/2\sigma^2}$ (and obviously by $\cos^2\Phi\sin^2\Phi e^{-\Phi^2/2\sigma^2}$) in the interval $[0, 2\pi]$ is the same as in the interval $[-\pi/2, 3\pi/2]$, as one can easily verify by plotting the functions. This rigorously establishes the identity $f_{GD}^{az} \equiv f_{GD}^{\{\frac{\pi}{2},0\}} = f_{GD}^{\{\frac{\pi}{2},\frac{\pi}{2}\}}$ which holds in the calculation of $\langle n_{ij}^x n_{ij}^y n_{ij}^x n_{ij}^y \rangle_{GD}$. With analogous arguments it is easy to show that $f_{GD}^{\{\frac{\pi}{2},0\}} = f_{GD}^{\{\frac{\pi}{2},p\pi/2\}}$ also holds $\forall p$ where p is an integer. This leads us to conclude that:

$$\sum_{p=0}^3 f_{GD}^{\{\frac{\pi}{2},p\frac{\pi}{2}\}} = 4f_{GD}^{az} \qquad (B12)$$

To complete the derivation of Eq.(B7) (i.e. Eq.(2) in the main article), we still need to demonstrate that $\sum_{q=0}^1 f_{GD}^{\{q\pi,\forall\phi\}} = 2f_{GD}^{ze}$ holds as well in the calculation of the angular average. The principal zenithal orientation f_{GD}^{ze}, with $q = 0$, contributes to the angular average $\langle n_{ij}^x n_{ij}^y n_{ij}^x n_{ij}^y \rangle_{GD}$ the following integral:

$$\int_0^\pi \sin^5\theta e^{-\theta^2/2\sigma^2} d\theta \int_0^{2\pi} \cos^2\phi\sin^2\phi d\phi \qquad (B13)$$

where we omitted again the normalization factor. The orientation with $q = 1$ gives the following contribution to the angular average:

$$\int_0^\pi \sin^5\theta e^{-(\theta-\pi)^2/2\sigma^2} d\theta \int_0^{2\pi} \cos^2\phi\sin^2\phi d\phi \qquad (B14)$$

This integral, upon changing to the variable $\Theta \equiv \theta - \pi$, becomes:

$$\int_{-\pi}^0 -\sin^5\Theta e^{-\Theta^2/2\sigma^2} d\Theta \int_0^{2\pi} \cos^2\phi\sin^2\phi d\phi \qquad (B15)$$

where we used $\sin(\theta - \pi) = -\sin\theta$. The function $\sin^5\Theta e^{-\Theta^2/2\sigma^2}$ is an odd function of the variable Θ. This implies that: $\int_{-\pi}^0 -\sin^5\Theta e^{-\Theta^2/2\sigma^2} d\Theta = \int_0^\pi \sin^5\Theta e^{-\Theta^2/2\sigma^2} d\Theta$. The last identity establishes that the integral in Eq.(B14) and the integral in Eq.(B13) are identical. This result in turn demonstrates that, for the purpose of calculating $\langle n_{ij}^x n_{ij}^y n_{ij}^x n_{ij}^y \rangle_{GD}$:

$$\sum_{q=0}^1 f_{GD}^{\{q\pi,\forall\phi\}} = 2f_{GD}^{ze}. \qquad (B16)$$

Recollecting the results presented above, we have shown rigorously that to the effect of calculating $\langle n_{ij}^x n_{ij}^y n_{ij}^x n_{ij}^y \rangle_{GD}$ the following equality holds:

$$f_{GD} = \frac{1}{6}\left(\sum_{p=0}^3 f_{GD}^{\{\frac{\pi}{2},p\frac{\pi}{2}\}} + \sum_{q=0}^1 f_{GD}^{\{q\pi,\forall\phi\}}\right) = \frac{4}{6}f_{GD}^{az} + \frac{2}{6}f_{GD}^{ze}$$

$$= \frac{4}{6}N_{az}(\sigma^2)e^{-(\theta-\frac{\pi}{2})^2/2\sigma^2} e^{-\phi^2/2\sigma^2} + \frac{2}{6}N_{ze}(\sigma^2)e^{-\theta^2/2\sigma^2}$$

$$(B17)$$

which has been used in the main article.

As shown in Fig.2 of the main article, using Eq.(??) to evaluate $\langle n_{ij}^x n_{ij}^y n_{ij}^x n_{ij}^y \rangle_{GD}$ leads us to recover exactly $\lim_{\sigma\to\infty}\langle n_{ij}^x n_{ij}^y n_{ij}^x n_{ij}^y \rangle_{GD} = 1/15$ which is the value that one calculates assuming that the bond orientations are randomly distributed in the solid angle, i.e. using the uniform-disorder ODF: $f_{UD} = 1/4\pi$. This result gives a further confirmation of the correctness of the above derivation.

Appendix C. Simulation of non-affine disordered lattices

We simulate the effect of non-affine deformations on the shear modulus of an elastic solid by implementing the following scheme. First we place N points on a perfect simple cubic lattice, then we perturb the lattice topology to induce a variable degree of disorder and we assign a harmonic elastic energy to each bond. Finally we deform the lattice by implementing a gradient descent method at zero-temperature to find the local energy minima.

Typically we choose a lattice composed of $20 \times 20 \times 20$ atoms corresponding to $N = 8000$, having confirmed that the intrinsically intensive value of the modulus has saturated on increasing N. Each point is then perturbed from its lattice position by drawing three random samples from a Gaussian distribution of variance and displacing the position of each atom by these values in the x, y and z directions. This process is repeated independently for each of the N atoms. We enforce the condition that all positions must be in the interval $[0, N]$ so that all positions x, y, z are, in fact, $modulo(x, N)$, $modulo(y, N)$, and $modulo(z, N)$. Once the positions of the vertices have been defined as above, the connections in the network are introduced by picking a vertex at random and forming bonds to each of the z nearest neighbors, provided they do not already have z neighbors, i.e. they are available. This process is repeated until the network is fully formed and no more bonds can be placed. This completely defined the topology of the network. The surfaces would usually present a problem for this method of forming connections since at the surface the nearest neighbors are predominantly 'behind' the atom in question. We overcome this difficulty by employing periodic boundary conditions. For instance, a vertex in the 'front' $y-z$ surface, that is, a vertex with $x \geq 0$ can connect to vertices in the 'back' $y-z$ surface $(x \geq L)$ by connecting forwards. In essence, instead of there being a single network, there is a central network (in which we form connections), but

this network is surrounded by 26 'image networks' which connect to the 6 faces, 12 edges and 8 corners such that connections from the central network can connect to a vertex in any one of the 26 surrounding networks if they happen to be one of the z nearest neighbors. In this way connections are not biased at the surfaces. Once the topology of the network is defined in this way, we deform the network affinely by a very small shear strain with typically $\epsilon = 10^{-4}$ (or $\epsilon = 0.01\%$). After the affine deformation we define a non-affine box, which is centered on the centre of the original network but extends out to 90% of the distance in the x,y,z directions compared to the original network. Each bond on a vertex exerts a force according to Hooke's law. If a vertex lies inside the non-affine box, the position is permitted to move under the influence of the force in an over-damped way (the time-step update is such that the positions are altered in the direction of, and with a magnitude proportional to, the force). All vertices outside the non-affine box, are not permitted to move and must therefore deform affinely. It is via these surface vertices that the strain constraint is implemented. This relaxation procedure is repeated 104 times and the energy of the network inside the non-affine box is recorded as E^{NA}. Each such relaxation procedure is repeated multiple times for each value of disorder. The shear modulus of the network is then inferred from this using the formula: $G = 2E^{NA}/\epsilon^2$, where we have assumed that the contributions to the modulus from the terms on the order of ϵ^4 can be neglected at deformations this small.

Many of theoretical results in this paper hold in the limit of large system size. To verify that the effects observed in our simulations are not merely finite size effects we repeated the simulations over a wide range of system sizes ($N_{min} = 64$, $N_{max} = 8000$), and observed that, as the system size increases, the curves of modulus against disorder approach saturation in a smooth manner, which we assume is the limit of infinite system size. Figure 3a in the main text illustrates this convergence.

The method of relaxation used in our simulations necessarily means that one will never truly reach equilibrium in a finite number of time-steps; at best the energy will approach its true equilibrium value exponentially. To test that the effects observed in this paper were not an artefact of incomplete relaxation of local forces, we similarly plotted the curves of modulus against disorder for increasing number of relaxation steps (equivalent to the time allowed for stress relaxation), ranging from 10 up to 10^5 in powers of $10^{1/2}$. Figure 3b in the main text illustrates this convergence. As in the case of finite size effects, the effect of finite relaxation time is that upon increasing the total number of steps, the curves converge smoothly to a limit which we take as the infinite-time one. We are therefore confident that neither finite size, nor finite time effects are responsible for the observed stiffening of network with disorder, but that the effect is an inherent property of the network.

[1] Alexander, S. Amorphous solids: their structure,lattice dynamics and elasticity. Phys. Rep. 296, 65 (1998).

[2] DiDonna, B. A. and Lubensky, T. C. Nonaffine correlations in random elastic media. Phys. Rev. E 72, 066619 (2005).

[3] Lemaitre, A. and Maloney, C. Sum Rules for the Quasi-Static and Visco-Elastic Response of Disordered Solids at Zero Temperature. J. Stat. Phys. 123, 415 (2006).

[4] Tanguy, A. et al. Continuum limit of amorphous elastic bodies: A finite-size study of low-frequency harmonic vibrations. Phys. Rev. B 66, 17 (2002).

[5] Utter, B. and Behringer, R.P. Experimental measures of affine and nonaffine deformation in granular shear. Phys. Rev. Lett. 100, 208302 (2008).

[6] Anderson, P.W. More is different - broken symmetry and nature of hierarchical structure of science. Science 177, 393 (1972).

[7] Anderson, P.W. in Ill-Condensed Matter, Les Houches Session XXXI, Eds. Balian, R., Maynard, R., and Toulouse, G. (North-Holland, Amsterdam, 1979).

[8] van Hecke, M. Jamming of soft particles: geometry,mechanics, scaling and isostaticity. J. Phys.: Cond. Mat. 22, 033101 (2010).

[9] Debenedetti, P.G. and and Stillinger, F.H. Supercooled liquids and the glass transition. Nature 410, 259 (2001).

[10] Feng, S., Thorpe, M. F. and Garboczi, E. Effective-medium theory of percolation on central-force elastic networks. Phys. Rev. B 31, 276 (1985).

[11] He, H. and Thorpe, M. F. Elastic properties of glasses. Phys. Rev. Lett. 54, 2107 (1985).

[12] Das, M., MacKintosh, F.C. and Levine, A.J. Effective medium theory of semiflexible filamentous networks. Phys. Rev. Lett. 99, 038101 (2007).

[13] C. Heussinger and E. Frey, Phys. Rev. Lett. **96**, 017802 (2006).

[14] Born, M. and Huang, H. The Dynamical Theory of Crystal Lattices, p.248 (Oxford University Press, Oxford, 1954).

[15] Phillips, J.C. and Thorpe, M.F. Constraint theory, vector percolation and glass-formation. Sol. State Commun. 53, 699 (1985).

[16] Yabuuchi, T. et al. New high-pressure phase of calcium. J. Phys. Soc. Japan 74, 2391 (2005).

[17] Djohari, H., Milstein, F. and Maroudas, D. Stability of simple cubic crystals. Appl. Phys. Lett. 90, 161910 (2007).

[18] Legut, D., Friak, M. and Sob, M. Why is polonium simple cubic and so highly anisotropic? Phys. Rev. Lett. 99, 016402 (2007).

[19] Zaccone, A. and Scossa-Romano, E. Approximate analytical description of the nonaffine response of amorphous solids. Phys. Rev. B 83, 184205 (2011).

[20] Makse, H. A., Gland, N., Johnson, D.L. and Schwartz, L.M. Why Effective Medium Theory Fails in Granular Materials. Phys. Rev. Lett. 83, 5070 (1999).

[21] O'Hern, C.S. et al. Jamming at zero temperature and zero applied stress: The epitome of disorder. Phys. Rev. E 68, 011306 (2003).

[22] Mao, X., Xu, N. and Lubensky, T.C. Soft Modes and Elas-

ticity of Nearly Isostatic Lattices: Randomness and Dissipation. Phys. Rev. Lett. 104, 085504 (2010).

[23] Obukhov, S. First-order rigidity transition in random rod networks. Phys. Rev. Lett. 74, 4472 (1995).

[24] Moukarzel, C., Duxbury, P.M. and Leath, P.L. Infinite-cluster geometry in central-force networks. Phys. Rev. Lett. 78, 1480 (1997).

[25] Wyart, M. On the rigidity of amorphous solids. Ann. Phys. (Paris) 30, 1 (2005).

[26] Steinhardt, P.J., Nelson, D.R. and Ronchetti, M. Bond-orientational order in liquids and glasses. Phys. Rev. B 28, 784 (1983).

[27] Debenedetti, P. G. Metastable Liquids (Princeton University Press, Princeton NJ, 1996).

[28] Jonsson, H. and Andersen, H.C. Icosahedral ordering in the Lennard-Jones liquid and glass. Phys. Rev. Lett. 60, 2295 (1988).

[29] Angell, C.A. Spectroscopy simulation and scattering, and the medium range order problem in glass. J. Non-Cryst. Solids 73, 1 (1985).

[30] Phillips, J. C. Topology of covalent non-crystalline solids 2. Medium-range order in chalcogenide alloys and a-Si(Ge) J. Non-Cryst. Solids 43, 37 (1981).

[31] Sheng, H.W. et al. Atomic packing and short-to-medium-range order in metallic glasses. Nature 439, 419 (2006).